Underwater oblique shock wave reflection

Ritwik Ghoshal*
Department of Civil and Environmental Engineering, Indian Institute of Technology Patna, Patna 801103, India

Nilanjan Mitra†
Department of Civil Engineering and Center for Theoretical Studies, Indian Institute of Technology Kharagpur, Kharagpur 721302, India

(Received 2 January 2017; published 29 January 2018)

This paper presents a comprehensive theoretical study of oblique shock wave reflection in water. The study identifies wedge angles in a structure that can alter the reflection characteristics of shock waves of different strengths. Utilizing the shock polar diagrams for both incident and reflected shock, the domain of regular and irregular reflection is identified. The effect of phase transition of water on reflection characteristics and its subsequent effect on the domain of regular and irregular reflection are also investigated theoretically. Results are compared between two equations of state, and it is observed that they give similar results for low-pressure regimes; however, reflection characteristics are significantly different for high-pressure regimes where phase transition of water has been reported to be observed. The implications of these theoretical observations are substantial for designing experimental devices and can be utilized to benchmark numerical simulations.

DOI: 10.1103/PhysRevFluids.3.013403

I. INTRODUCTION

There are numerous papers on shock wave reflection in an air medium, including both experimental and theoretical studies. However, for a water medium, the literature appears to be very limited. Typically water is taken as a nearly incompressible medium, and any shock waves through it are usually considered within the acoustic approximation. It should be noted, however, that some studies have reported both experimentally [1–9] and numerically [10–12] that water under shock and/or static compression undergoes a phase transition, which definitively indicates that under conditions of high pressure water may not demonstrate an isochoric behavior, thereby dispelling the assumption of an incompressible medium for water.

The word "shock" typically refers to a discontinuity traveling through a medium. Shocks are macroscale abstractions of very fast molecular and atomic processes occurring over a very thin region in space. Shock loading typically refers to a sudden increase in pressure (along with temperature in many situations) for a very short time duration. The behavior of water subjected to extreme pressure and temperature is of profound importance in planetary science [13], geochemistry [14], and fundamental chemistry [4,15]. Apart from these studies, an interesting area of painless drug delivery is being researched which involves collapse of cavitation nanobubbles in water resulting in formation of shock waves [16]. It should be understood that underwater explosion-induced shock wave loading on structures with inclined surfaces (e.g., gravity dams, gravity platforms, foundation

*ritwik.ghoshal@gmail.com
†nilanjan@civil.iitkgp.ernet.in

of offshore structures, wind turbines, ship structures etc.) can transpire in situations of oblique reflection. Therefore, it is imperative to develop an understanding of oblique shock wave reflection in water, which this paper addresses from a theoretical perspective. It should also be understood that because of differences in molecular structure and energy associated with the atoms, an argument that the study of shock wave reflection in air is very similar to that of an underwater situation does not hold properly. See the book by Ben-Dor [17] (and references therein) for a detailed exposition of the topic of shock wave propagation and reflection in air.

With regard to underwater shock wave propagation and reflection, a comprehensive review of large-scale experiments and modeling of the phenomena was reported by Cole [18] and Swisdak [19]. It is worth mentioning that oblique reflection of underwater explosion-induced shock and its implications on blast mitigation is an area that has not been rigorously explored. Ridah [20] theoretically demonstrated the detachment criteria and sonic criteria for an oblique shock in water using the Tait equation of state (EoS) for compressible water medium. It should be noted that the Tait EoS is a barotropic EoS which can model only isentropic flows. However, when there is a shock wave in a medium, the physical meaning of the assumption that entropy is constant along a shock front is unrealistic, and thereby the use of the Tait EoS is questionable. Moreover, the Tait EoS assumes a constant pressure contribution for the lattice configuration part, which does not provide good results for high-pressure ranges. It has been reported that the Tait EoS does not give good representation of pressure beyond 25 kbar [20]. In high-pressure regimes, where a phase transition is also observed, the use of the Tait EoS is also questionable. The Tait EoS has also been reported not to provide good results for regions where cavitation is observed as a result of fluid-structure interaction [21]. However, since this is a well-known EoS for water and has been used previously in the literature for underwater shock wave reflection, this EoS has also been considered in this study for comparison.

A detailed characterization of shock strengths and angles to identify the domains of regular and irregular reflections in water medium cannot be obtained from current literature [20]. The necessity of considering water as a compressible medium instead of an incompressible medium from the viewpoint of underwater shock loading was stressed by Ridah [20] and later by the authors [22]. Ridah [20] mentioned that nonlinear compressibility effects in water should be considered even for high-speed water jets in which the particle velocities may reach up to 1 km/s. Ghoshal and Mitra [22] highlighted the implications of nonlinear compressibility of water for underwater explosion-induced shocks with normal incidence and eventually developed a new theory extending Taylor's theory to high-intensity explosive loading as well as for near noncontact underwater shock wave loading situations. The need of considering a nonlinear compressible medium was also pointed out in Ref. [23] for deep underwater situations even for small peak over-pressures. Nadamitsu *et al.* [24] studied von Neumann reflection in underwater shock and demonstrated good agreement between analytical, numerical, and experimental investigations. However, their work is limited to some specific angles and very small peak pressures.

In the present work, a comprehensive theoretical study is carried out to investigate the domains of regular and irregular reflection of an underwater oblique shock wave, arising from different transition criteria, *viz.,* detachment criteria, sonic incident criteria, and mechanical equilibrium criteria. Since water under dynamic shock compression exhibits solidlike behavior [25], a Mie-Grüneisen equation of state (MGEoS) is used to model the nonlinear compressible water medium, and therefore this theory is applicable to very high-pressure ranges as well as in situations involving cavitation-induced shock loads and/or phase transition. Comparisons of results obtained from the MGEoS are also made with the Tait EoS. It should also be pointed out that the response for shock compressions in air is significantly different from the current study since those studies consider the gaseous behavior of the medium being represented by either ideal gas EoS (for low shock intensities) or real gas EoS [26].

II. ANALYTICAL PROBLEM FORMULATION

Underwater shock wave reflection from a fixed or rigid wall with a V-shaped appendage at the front side is studied here to analytically determine the flow variables of the shocked states and

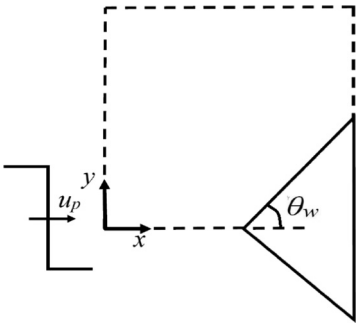

FIG. 1. Schematic illustration of the problem of oblique shock reflection from a V-shaped fixed rigid structure.

the transition lines of different shock reflection domains. The V-shaped appendage is considered as nondeformable (i.e., rigid), thereby having infinite acoustic impedance. Since the acoustic impedance of water is much larger than that of air and is often comparable to solid structures, there arise fluid-structure-interaction (FSI) problems in many cases. To ignore FSI, there is a need to introduce the rigid wall assumption. In Fig. 1 a schematic description of the problem is provided along with the flow field representing oblique underwater shock wave reflection from a fixed or rigid V-shaped appendage. Rankine-Hugoniot jump (RHJ) conditions for oblique shock along with the MGEoS or the Tait EoS is utilized to determine a closed form solution of the flow variables in a discontinuous hyperbolic system of partial differential equations [27,28].

In the case of a two-dimensional inviscid flow, RHJ conditions for an oblique shock take a form as follows. Mass conservation gives

$$\rho_i U_i \sin\phi_j = \rho_j U_j \sin(\phi_j - \theta_j). \tag{1}$$

Linear momentum conservation (normal and tangential to the shock front) gives

$$p_i + \rho_i U_i^2 \sin^2\phi_j = p_j + \rho_j U_j^2 \sin^2(\phi_j - \theta_j), \tag{2}$$

$$\rho_i \tan\phi_j = \rho_j \tan(\phi_j - \theta_j). \tag{3}$$

Energy conservation gives

$$e_i + \frac{p_i}{\rho_i} + \frac{1}{2}U_i^2 \sin^2\phi_j = e_j + \frac{p_j}{\rho_j} + \frac{1}{2}U_j^2 \sin^2(\phi_j - \theta_j). \tag{4}$$

Here U represents shock velocity measured with respect to a reference frame attached to the shock front. Flow states ahead and behind the shock are represented by index i and j, respectively. Internal energy, pressure, and fluid density are symbolized by e, p, and ρ, respectively. The angle between direction of incident flow and the oblique shock front is ϕ_j, whereas θ_j represents the flow deflection angle. Assuming a thermodynamic equilibrium between upstream and downstream of shock, RHJ conditions can be solved with the help of an EoS, $p = p(\rho,e)$.

The Tait EoS was originally proposed to model the compressibility of water. Kirkwood and Bethe [18] provided a modification to the Tait EoS. For the Tait EoS, the thermodynamic part is

$$p = B(\mathcal{S})\left[\left(\frac{\rho}{\rho_0}\right)^{\gamma_w} - 1\right] + p_0 \tag{5}$$

and the caloric part is

$$e = \frac{B(\mathcal{S})\rho^{\gamma_w - 1}}{(\gamma_w - 1)\rho_0^{\gamma_w}} + \frac{B - p_0}{\rho}. \tag{6}$$

Here $B(\mathcal{S})$ is a parameter which is a function of entropy and γ_w is a constant. The value of $B(\mathcal{S})$ is generally taken as 3047 bar calculated for 0.7 molal salt water at 20 °C. Constant γ_w has a value of 7.15. It should be noted that in many analyses variation of entropy is neglected, and hence B turns out to be constant. This essentially converts the Tait EoS to a barotropic EoS, i.e., pressure is only a function of density, $p = p(\rho)$. Therefore, the energy equation becomes unnecessary while solving RHJ conditions using the Tait EoS. In this context, it should be mentioned that the Tait EoS is an empirical equation of state with little theoretical justification, and it gives excellent representation for a pressure range up to 25 kbar [20]. However, for a pressure range beyond 25 kbar where phase transition of water has been reported [20], the Tait EoS is no longer valid. Therefore, in the present work the MGEoS is used for modeling a nonlinear compressible water medium, and the Tait EoS is utilized as a reference. Here, it should be noted that here the structure is assumed to be rigid-stationary, and thus fluid never undergoes tension, i.e., cavitation does not occur upon reflection. Hence, the MGEoS for the compression phase is used for all calculations, given as

$$p = \frac{\rho_0 c_0^2 \mu\left[1 + \left(1 - \frac{\Gamma_0}{2}\right)\mu\right]}{[1 - (S-1)\mu]^2} + \Gamma_0 \rho_0 e, \tag{7}$$

where Γ_0 is the Grüneisen parameter at the initial state. The MGEoS is developed based on an experimentally determined Hugoniot curve, which refers to the shock-particle velocity (U_s-u_p) relationship. In the present work, the shock particle velocity relation provided by Bogdanov [8] is used. These shock-particle velocity data were supported by various other researchers as well [9,29]. Some of the recent works based on molecular dynamics also reported similar results [10]. Therefore, the results provided here are unique to that of water. This shock-particle velocity (U_s-u_p) relation consists of three discrete linear segments and considers the effect of the phase change of water at high pressure. The fitting coefficients of the linear shock-particle velocity relationship, c_0 and S, are taken as 1450 and 2.166, 1879 and 1.68, and 2963 and 1.185 for phases I, II, and III, respectively. For an oblique shock, the linear shock-particle velocity relationship can be written as

$$U_{sn} = c_0 + S u_{pn}, \tag{8}$$

where U_{sn} and u_{pn} are the components normal to the shock front of shock (U_s) and particle velocity (u_p), measured in a reference configuration.

Flow variables downstream of the incident shock are obtained by solving the RHJ condition along with an EoS, applied between the shocked and unshocked zone. Properties of unshocked water are chosen to be those of the ambient condition. Incident shock quantities ($\rho_1, p_1, e_1, \theta_1$) are determined for an incident shock velocity (U_0) and shock angle (ϕ_1).

Once the incident shock quantities are obtained, reflected shock quantities (ρ_2, U_2, e_2, p_2) can also be obtained by again solving the RHJ condition along with an EoS, applied between reflected and incident shock.

Combining these equation yields a fourth degree polynomial of $\tan\theta_2$. Solving this polynomial (for detail derivation see Ref. [30]) for a given incident shock state (p_1, ϕ_1), θ_2 is calculated for various values ϕ_2. Only the real positive root within the range $0 \leqslant \theta_2 \leqslant 90$ is considered. Using θ_2, reflected shock quantities (ρ_2, U_2, e_2, p_2) can be obtained, and consequently the reflected shock polars are drawn.

The shock polar solution for regular and irregular reflection can be obtained from the theory presented above. These shock polar solutions are utilized to graphically determine transition lines arising from different criteria for regular and irregular reflection in a water medium.

A. Mach wave condition

A Mach wave condition (MWC), i.e., the upper boundary of the shock reflection domain, is given as

$$\phi|_{MWC} = \sin^{-1}\left(\frac{c_0}{U_{sn}}\right), \tag{9}$$

where c_0 is the sound speed in water medium. No incident shock can exist at an angle less than an angle given by this condition. The plate angle from Mach wave condition can be obtained as $\theta_w|_{MWC} = 90^\circ - \phi|_{MWC}$.

B. Sonic incident condition

A shock reflection is not possible if the downstream of the shock is subsonic, which sets the upper boundary of the reflection domain. The limiting value of the incident angle ($\phi|_{SIC}$) i.e., sonic incident criteria (SIC), should satisfy the following condition:

$$\phi = \phi|_{SIC} \text{if} \frac{c_1}{u_1} < 1, \tag{10}$$

where c_1 and u_1 are the sound speed and shock velocity downstream of the incident shock. u_1 can be obtained by solving RHJ condition applied between the shocked and unshocked zone. The sound speed downstream of the shock can be obtained using the following relation as

$$c^2 = \left(\frac{\partial p}{\partial \rho}\right)_e + \frac{p}{\rho^2}\left(\frac{\partial p}{\partial e}\right)_\rho. \tag{11}$$

The plate angle for sonic incident condition is given as $\theta_w|_{SIC} = 90^\circ - \phi|_{SIC}$.

C. Detachment condition

The detachment condition (DC) for a given Mach number is defined as the incident shock angle at which the maximum flow turning angle by the reflected shock equals the flow turning angle of the incident shock. For a shock angle larger than that at the detachment condition, regular reflection is not possible. The detachment condition for an incident shock angle ($\phi|_{DC}$) can be obtained when the flow turning angle of the incident shock and the maximum flow deflection angle of the reflected shock are the same. Subsequently, the plate angle for detachment condition can be obtained as $\theta_w|_{DC} = 90^\circ - \phi|_{DC}$.

D. Mechanical equilibrium condition

The transition line of mechanical equilibrium criteria, which is also known as von Neumann criteria, can be obtained using the three-shock theory, and this requires satisfying the following condition:

$$\theta_1 - \theta_2 = \theta_3 = 0. \tag{12}$$

Here θ_1, θ_2, and θ_3 are the flow deflection angle at the incident, reflected, and Mach-stem region. The incident shock angle ($\phi|_{vN}$) for the mechanical equilibrium condition can be obtained when the reflected shock polar intersects the p axis at the normal shock point of the incident shock polar. Therefore, the plate angle for von Neumann criteria is given as $\theta_w|_{vN} = 90^\circ - \phi|_{vN}$.

Transition curves separating different shock reflection domains obtained through these conditions are plotted in the next section for different shock intensities. Uniform shocks of various strengths impinging on a plate with a V-shaped appendage of various angles are studied. For all calculations presented here the initial pressure (p_0) is taken as the hydrostatic pressure (p_{hyd}) at a water depth of 1.5 m: $p_0 = p_{atm} + p_{hyd}$. The atmospheric pressure (p_{atm}) is taken as 1.013 bar. The initial internal energy (e_0) corresponding to the chosen ambient condition is obtained from the corresponding EoS. Initial density is taken as $1000\,\text{kg/m}^3$.

III. RESULTS AND DISCUSSION

Figure 2(a) presents four different shock reflection domains, which are obtained using the transition criteria based on the different EoS (presented in the previous section). Lines obtained from different criteria (MWC = Mach wave criterion, DC = detachment criterion, SIC = sonic

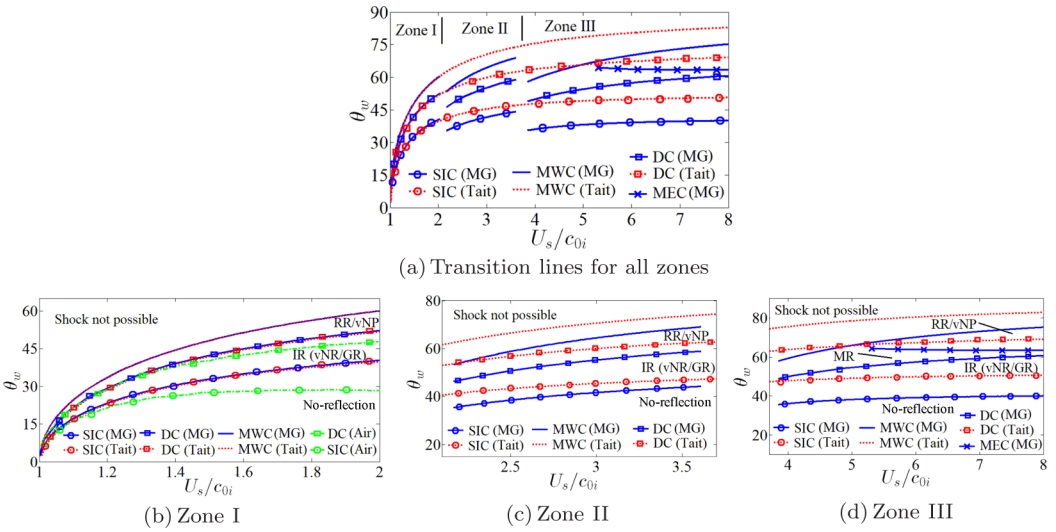

(a) Transition lines for all zones

(b) Zone I

(c) Zone II

(d) Zone III

FIG. 2. Transition lines arising from different criteria for oblique shock reflection in a water medium.

incident criterion) separating different regions of shock wave reflection (no-reflection, irregular reflection, regular reflection, shock not possible) are shown in the figure for both EoSs employed here. Three different zones, as per demarcations in Ref. [8], have been represented in these curves. A detailed comparison is presented in Figs. 2(b), 2(c), and 2(d) for the three zones respectively along with similar characterization for oblique air-shock loading, considering ideal gas an EoS (which also can be obtained directly from the literature [17,31,32]). In zone I [see Fig. 2(b)] both the Tait EoS and the MGEoS give similar results, whereas differences are observed in the other zones [see Figs. 2(c) and 2(d)]. This is quite obvious since the fitting coefficients of the linear shock-particle velocity relationship are varied for the MGEoS in the different zones, while no such measures can be employed for the Tait EoS. Here it should be noted that shock velocities are normalized with respect to the initial sound speed of the medium c_{0i}, and hence, it corresponds to the value of c_0 for zone I, whereas for air it is taken as 346 m/s.

In the region of no-reflection the shock wave will not result in any reflection from the structure but would instead glide along the profile of the structure. Typically this angle (which separates a region of no-reflection of shock waves to that where reflected shocks could be observed) is dependent upon the strength or intensity of the incident shock wave (being determined with the increase in piston velocity). In region I [see Fig. 2(b)], this separation line increases (in a nonlinear manner) with that of the incident shock strength. Differences could be observed between regions of no-reflection for the case of air and water medium. For a water medium the wedge angles are higher compared to that of the air medium. Here it should be noted that apart from molecular differences between an air and water medium, the density of water is almost 10^3 times that of air, and therefore, pressure, temperature, and material or shock velocity in a water medium are significantly high compared to that of an air medium. Next is the region where the regular reflection is impossible. This means that the shock reflection observed in this region is irregular in nature. The nature of the irregular reflections can be either Mach reflection, von Neumann reflection, or Guderley reflection. In fact, for the range of piston velocities considered here for the water medium, we observe von Neumann reflection with a subsonic downstream in this regime. A comparison of this region for an air and water medium shows that the region for a water medium is much narrower compared to that of the air medium. Moreover, higher wedge angles are required in a water medium to observe regular reflection. Transition to irregular reflection occurs when the deflection achievable by a reflected shock is insufficient to turn the flow back to a direction parallel to the incident flow, which in turn results in formation of a triple point with

the incident and reflected shock. Here it should be noted that water being a denser fluid, the transition from the regular to the irregular reflection is significantly different compared to that of air. It should be noted also that the type of irregular reflection for that of an air medium is also different compared to that of water. In air a von Neumann reflection or Guderley-type reflection was reported to be observed for normalized shock velocity $U_s/c_{0i} < 1.25$, whereas for $U_s/c_{0i} > 1.48$ Mach reflections [subsonic flow downstream of the reflected shock (MRs) or Mach reflection with a forward-facing reflected shock (MRf)] were reported [17]. Above this region is the region where regular reflections may be possible; in fact, in this region, regular reflections with subsonic downstream are observed for the case of a water medium. In the case of an air medium, discrepancies between von Neumann's classical theory and experimental results were reported for the ranges of U_s/c_{0i} considered here. This phenomenon is well known as the von Neumann paradox [33], which is still an unsolved topic in the realm of air-shock reflections. Therefore, an extensive study based on experiments is required to properly identify this phenomenon in the water medium and can be considered as an extension of this work. Above this region it is observed that the horizontal component of the velocity of the incident shock is below the sonic velocity in the medium; thereby this region is classified as a "shock not possible" region. It should be pointed out that this line for the air and water medium (for both EoSs) coincides with each other.

In zone II, significant deviation can be observed between the transition lines arising from the MGEoS and Tait EoS, as depicted in Fig. 2(c). Typically the MGEoS demonstrates lower wedge angles compared to the Tait EoS for similar Mach numbers. The differences between the transition lines obtained from the two different EoSs can be attributed to the effect of a phase transition, which is considered in the MGEoS through the incorporation of different coefficients (c_0 and s) for different phases in Eq. (7). This has been discussed previously, and the physical justification for change in the slope of the U_s-u_p curve is because of observance of the solid phase of water (ice VII) under shock compression [3,8,10]. Furthermore, the barotropic assumption in the Tait EoS renders itself independent of internal energy, which may not be a valid assumption at a high pressure range, especially in the presence of a phase transition. In Fig. 2(c) comparison with air is not provided [unlike Fig. 2(b) and 2(d)], since an ideal gas assumption is no longer valid for these high Mach numbers (see Ref. [26]). It should be noted that the notion of a phase transition in water under normal shock compression is applied here for oblique shock reflection. Therefore, based on physical consideration that regions of phase transition will not alter due to oblique reflection, it may be argued that the MGEoS will give better correlation compared to the Tait EoS at high Mach numbers. It should be remembered that these investigations are purely theoretical, and exhaustive experimental investigations are warranted to verify these predictions.

Similar observations can be made for zone III [see Fig 2(d)]. It can also be observed that the gap between the DC and SIC line (also between the DC and MWC lines) for the MGEoS increases more in comparison to that for the Tait EoS, in which it remains almost constant. Furthermore, the Tait EoS does not produce a situation where a reflected shock polar intersects the p axis at the normal shock point of the incident shock polar; i.e., the mechanical equilibrium condition is never achieved using the Tait EoS for the range of particle velocities considered here. However, using the MGEoS, which accounts for phase transition effects at high pressure ranges, the transition line arising from a mechanical equilibrium condition can be obtained.

In order to properly identify the types of irregular and regular reflections (as observed in Fig. 2), shock polar diagrams are drawn for some shock velocities. A shock polar is defined as a locus of flow states obtained on passing through an oblique shock wave (represented in terms of pressure obtained and the angle by which the flow is deflected) for a specific particle velocity. An incident shock polar is determined by varying the angle of incidence (ϕ) (i.e., all possible solutions) in the RHJ condition applied between a shocked and unshocked zone. After that the reflected shock polar for a particular incident shock pressure and the incident angle are obtained by solving the RHJ condition applied between the reflected shock and incident shock.

As per the definition in the literature [17], a regular reflection (RR) wave configuration consists of two shock waves, the incident and the reflected shock wave, which meet at the reflection point

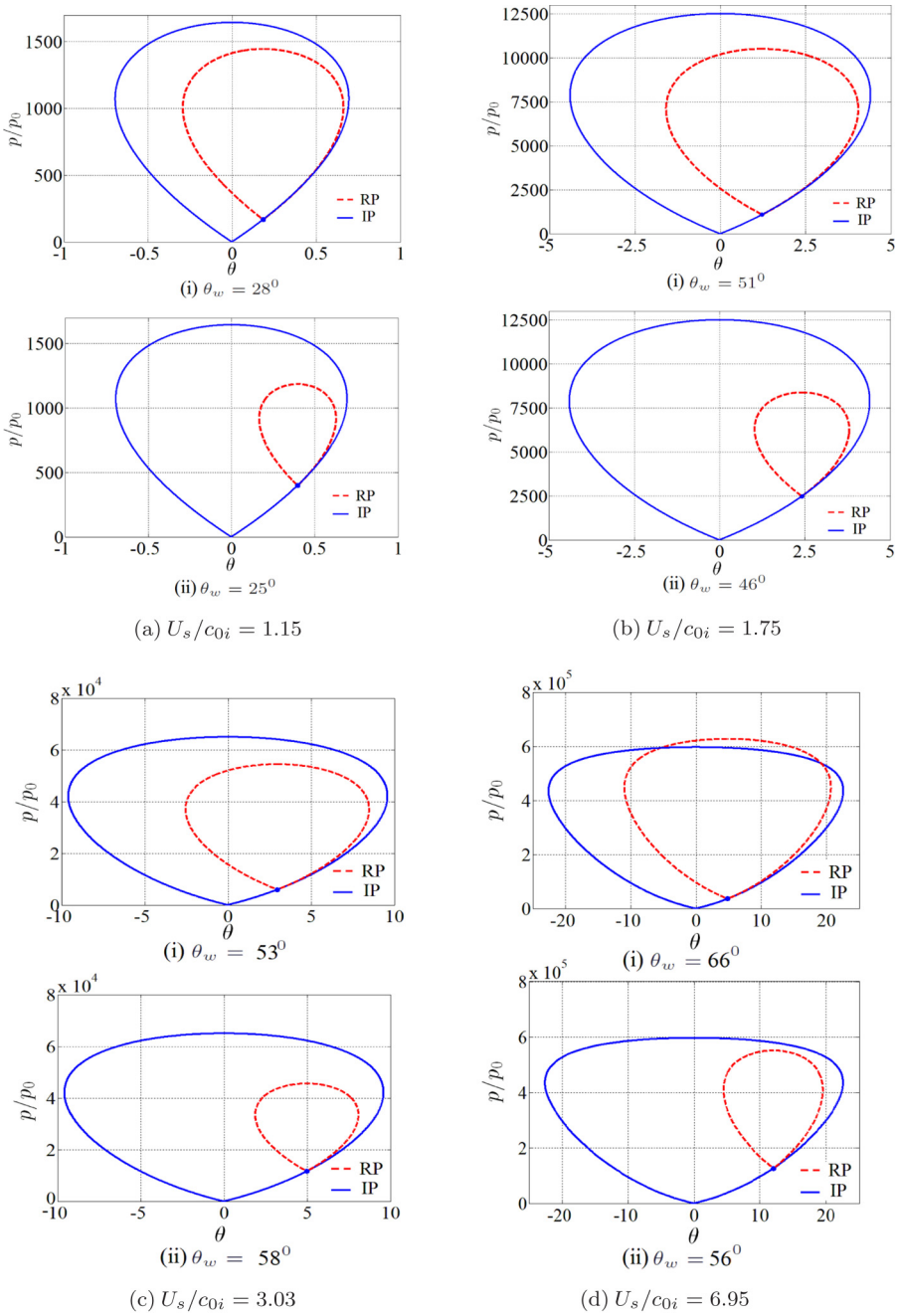

FIG. 3. Incident (IP) and reflected (RP) shock polar diagram for nondimensonal shock velocities (U_s/c_{0i}): (a) 1.15 ($u_p = 100$ m/s), (b) 1.75 ($u_p = 500$ m/s), (c) 3.03 ($u_p = 1500$ m/s), (d) 6.95 ($u_p = 6000$ m/s).

located on the reflecting surface. All other wave configurations are termed irregular reflections (IRs) (in which the triple point is located above the reflecting surface). This IR domain can further be subdivided into four subdomains: (1) a subdomain in which the three-shock theory of von Neumann has a "standard" solution ($\theta_1 - \theta_2 = \theta_3$ [17]) referred to a Mach reflection (MR); (2) the three-shock

theory has a "nonstandard" solution ($\theta_1 + \theta_2 = \theta_3$ [17]) referred to as von Neumann reflection (vNR); (3) a subdomain in which the three-shock theory does not have a solution but experimental evidence shows its presence, referred to as Guderley reflection (GR); and (4) a subdomain between vNR and GR termed Vasilev reflection (VR). A combination of vNR, GR, and VR is also referred to as a weak shock wave reflection domain. Typically the analytical equations can demonstrate the transition line between regular and irregular reflection but cannot demonstrate the subdivisions between the irregular reflections for which one needs to look into the IR shock polar diagrams. RR can ideally be observed if the reflected shock polar (RP) intersects the p axis and is not entirely encapsulated within the IR shock polar. If RP intersects the p axis and is entirely encapsulated within the incident shock polar (IP), then typically RP touches the IP at an angle greater than the initial angle, and hence it may be classified as a regular reflection with subsonic downstream; whereas if the RP is tangent to the p axis, then it represents the detachment criteria. On the other hand, if the RP does not touch the p axis and is entirely encapsulated within the IP, then it is termed vNR. If the RP does not intersect the p axis and is also not entirely encapsulated by the IP having points of intersection with the IP at angles lower than the initial angle, then it typically defines a proper MR. The shock polar for GR is not known even though it was observed experimentally by numerous researchers [17,33–35].

Figure 3 shows the shock polar diagrams for nondimensional Mach numbers (U_s/c_{0i}) of 1.15, 1.75, 3.03, and 6.95, respectively (these values correspond to a piston velocity of 100, 500, 1500, and 6000 m/s, respectively). The shock polar has been drawn based on using the MGEoS. For zone I, the similar nature of the curves is seen for $\theta_w = 25^\circ$ ($U_s/c_{0i} = 1.15$) and $\theta_w = 46^\circ$ ($U_s/c_{0i} = 1.75$) in which the reflected shock polar does not intersect the p axis and is entirely encapsulated by the incident shock polar, which demonstrate signatures of von Neumann reflection (as described above). On the other hand, for zone I, the similar nature of the curves are seen for $\theta_w = 28^\circ$ ($U_s/c_{0i} = 1.15$) and $\theta_w = 51^\circ$ ($U_s/c_{0i} = 1.75$) in which the reflected shock polar intersects the p axis but is entirely encapsulated by the incident shock polar, demonstrating signatures of regular reflection with subsonic downstream flow (as described above). Similar behavior like that in zone I can be observed for zone II ($U_s/c_{0i} = 3.03$), in which for $\theta_w = 53^\circ$ we observe von Neumann reflection and for $\theta_w = 58^\circ$ we observe a regular reflection with subsonic downstream. For zone III, von Neumann reflection is observed for $\theta_w = 56^\circ$, and conventional regular reflection (in which the RR intersects the p axis as well as the IR) is observed for $\theta_w = 66^\circ$.

IV. CONCLUSION

Underwater oblique shock wave reflection from fixed-rigid V-shaped appendage is studied in this paper analytically using the Mie-Grüneisen and Tait EoS. Utilizing the shock polar diagrams, transition lines arising from a Mach wave condition, sonic incident criteria, detachment criteria, and mechanical equilibrium criteria are identified for particle velocities ranging from 0 to 7 km/s for shock waves in a water medium. Since it has been reported that the Tait EoS is barotropic in nature and does not provide excellent representations for a pressure range above 25 kbar, this EoS cannot be used effectively for regions in which water undergoes a phase transition to ice VII. Utilizing the MGEoS, it is demonstrated that occurrence of a phase transition significantly influences the reflection characteristics. The analytical observations warrant verification by experimental observations and can also provide a benchmark for future numerical simulations.

ACKNOWLEDGMENTS

This work was carried out under the auspices of the Naval Research Board, India under Award No. NRB-226/HYD/10-11. Any opinions, findings, and conclusions or recommendations expressed in this paper are those of the writers and do not necessarily reflect those of the Naval Research Board, India.

[1] A. Vogel, S. Busch, and U. Parlitz, Shock wave emission and cavitation bubble generation by picosecond and nanosecond optical breakdown in water, J. Acoustic Soc. Am. **100**, 148 (1996).
[2] D. Dolan, J. Johnson, and Y. M. Gupta, Nanosecond freezing of water under multiple shock wave compression: Continuum modeling and wave profile measurements, J. Chem. Phys. **123**, 064702 (2005).
[3] D. Dolan, M. Knudson, C. Hall, and C. Deeney, A metastable limit for compressed liquid water, Nat. Phys. **3**, 339 (2007).
[4] Z. Men, W. Fang, D. Li, Z. Li, and C. Sun, Raman spectra from symmetric hydrogen bonds in water by high-intensity laser-induced breakdown, Sci. Rep. **4**, 4606 (2014).
[5] R. Hemley, A. Jephcoat, H. Mao, C. Zha, L. Finger, and D. Cox, Static compression of H_2O-ice to 128 GPa (1.28 Mbar), Nature (London) **330**, 737 (1987).
[6] A. Goncharov, V. Struzhkin, M. Somayazulu, R. Hemley, and H. Mao, Compression of ice to 210 gigapascals: Infrared evidence for a symmetric hydrogen-bonded phase, Science **273**, 218 (1996).
[7] C. G. Salzmann, P. G. Radaelli, A. Hallbrucker, E. Mayer, and J. L. Finney, The preparation and structures of hydrogen ordered phases of ice, Science **311**, 1758 (2006).
[8] G. Bogdanov and A. Rybakov, Anomalies of shock compressibility of water, J. Appl. Mech. Tech. Phys. **33**, 162 (1992).
[9] A. Rybakov, Phase transformation water under shock compression, J. Appl. Mech. Tech. Phys. **37**, 629 (1996).
[10] A. Neogi and N. Mitra, Shock induced phase transition of water: Molecular dynamics investigation, Phys. Fluids **28**, 027104 (2016).
[11] J. Aragones, M. Conde, E. Noya, and C. Vega, The phase diagram of water at high pressures as obtained by computer simulations of the TIP4P/2005 model: The appearance of a plastic crystal phase, Phys. Chem. Chem. Phys. **11**, 543 (2009).
[12] N. Goldman, E. J. Reed, I.-F. W. Kuo, L. E. Fried, C. J. Mundy, and A. Curioni, Ab initio simulation of the equation of state and kinetics of shocked water, J. Chem. Phys. **130**, 124517 (2009).
[13] L. K. M. Kanani, L. R. Benedetti, R. Jeanloz, P. M. Celliers, J. H. Eggert, D. G. Hicks, S. J. Moon *et al.*, Laser-driven shock experiments on precompressed water: Implications for "icy" giant planets, J. Chem. Phys. **125**, 014701 (2006).
[14] B. R. Simoneit, Aqueous high-temperature and high-pressure organic geochemistry of hydrothermal vent systems, Geochim. Cosmochim. Acta **57**, 3231 (1993).
[15] G. Walrafen, M. Hokmabadi, W. Yang, and G. Piermarini, High-temperature high-pressure Raman spectra from liquid water, J. Phys. Chem. **92**, 4540 (1988).
[16] M. Vedadi, A. Choubey, K. Nomura, R. K. Kalia, A. Nakano, P. Vashishta, and A. C. T. van Duin, Structure and Dynamics of Shock-Induced Nanobubble Collapse in Water, Phys. Rev. Lett. **105**, 014503 (2010).
[17] G. Ben-Dor, *Shock Wave Reflection Phenomena*, Shock Wave and High Pressure Phenomena (Springer, Berlin, 2007).
[18] R. H. Cole, *Underwater Explosions* (Princeton University Press, Princeton, NJ, 1948).
[19] M. M. Swisdak, Explosion effects and properties—Part II: Explosion effects in water, Technical Report, Naval Surface Weapons Center, Dahlgren, VA (1978).
[20] S. Ridah, Shock waves in water, J. Appl. Phys. **64**, 152 (1988).
[21] J. M. Richardson, A. B. Arons, and R. R. Halverson, Hydrodynamic properties of sea water at the front of a shock wave, J. Chem. Phys. **15**, 785 (1947).
[22] R. Ghoshal and N. Mitra, Non-contact near-field underwater explosion induced shock-wave loading of submerged rigid structures: Nonlinear compressibility effects in fluid structure interaction, J. Appl. Phys. **112**, 024911 (2012).
[23] R. Ghoshal and N. Mitra, Underwater explosion induced shock loading of structures: Influence of water depth, salinity and temperature, Ocean Eng. **126**, 22 (2016).
[24] M. F. Y. Nadamitsu, Z. Y. Liu, and S. Itoh, Von Neumann reflection of underwater shock wave, J. Mater. Process. Technol. **85**, 48 (1999).
[25] R. H. Wentorf, Jr., High pressure phenomena, in *Physical Chemistry: An Advanced Treatise*, edited by H. Eyring, D. Henderson, and W. Jost (Academic Press, New York, 1971), pp. 571–611.

[26] R. Ghoshal and N. Mitra, High-intensity air-explosion-induced shock loading of structures: Consideration of real gas in modeling of nonlinear compressible medium, Proc. R. Soc. Lond. A **471**, 20140825 (2015).
[27] J. Brown and G. Ravichandran, Analysis of oblique shock waves in solids using shock polars, Shock Waves **24**, 403 (2014).
[28] R. Menikoff and B. Plohr, The Riemann problem for fluid flow of real materials, Rev. Mod. Phys. **61**, 75 (1989).
[29] K. Nagayama, Y. Mori, Y. Motegi, and M. Nakahara, Shock Hugoniot for biological materials, Shock Waves **15**, 267 (2005).
[30] R. Ghoshal, Non-contact explosion induced shock wave response of structures, Ph.D. thesis, Indian Institute of Technology Kharagpur, 2015.
[31] H. Hornung, Regular and Mach reflection of shock waves, Annu. Rev. Fluid Mech. **18**, 33 (1986).
[32] C. Mouton and H. Hornung, Experiments on the mechanism of inducing transition between regular and Mach reflection, Phys. Fluids **20**, 126103 (2008).
[33] E. Tabak and R. Rosales, Focusing of weak shock waves and the von Neumann shock reflection, Phys. Fluids **6**, 1874 (1994).
[34] A. Defina, F. Susin, and D. Viero, Numerical study of the Guderley and Vasilev reflections in steady two-dimensional shallow water flow, Phys. Fluids **20**, 097102 (2008).
[35] E. Vasilev, T. Elperin, and G. Ben-Dor, Analytical reconsideration of the von Neumann paradox in the reflection of a shock wave over a wedge, Phys. Fluids **20**, 046101 (2008).